PROCEEDINGS OF SCIENCE

Solar and geo neutrinos in Borexino: summary of the Phase-I measurements and recent results

Gemma Testera*
Istituto Nazionale di Fisica Nucleare (Genova) Italy
E-mail: testera@ge.infn.it

On behalf of the Borexino Collaboration:

G. Bellini[h], D. Bick[q], G. Bonfini[e], D. Bravo[o], B. Caccianiga[h], F. Calaprice[k], P. Cavalcante[e], A. Chavarria[k], A. Chepurnov[p], D. D'Angelo[h], S. Davini[r],era A. Derbin[l], A. Etenko[g], K. Fomenko[b,e], D. Franco[a], C. Galbiati[k], C. Ghiano[a], M. Göger-Neff[m], A. Goretti[k], C. Hagner[q], E. Hungerford[r], Aldo Ianni[e], Andrea Ianni[k], V. Kobychev[f], D. Korablev[b], G. Korga[r], D. Kryn[a], M. Laubenstein[e], E. Litvinovich[g], F. Lombardi[e], P. Lombardi[h], L. Ludhova[h], G. Lukyanchenko[g], I. Machulin[g], S. Manecki[o], W. Maneschg[i], E. Meroni[h], L. Miramonti[h], M. Misiaszek[d], P. Mosteiro[k], V. Muratova[l], L. Oberauer[m], M. Obolensky[a], F. Ortica[j], K. Otis[n], M. Pallavicini[c], L. Papp[o], A. Pocar[n], G. Ranucci[h], A. Razeto[e], A. Re[h], A. Romani[j], N. Rossi[e], R. Saldanha[k], C. Salvo[c], S. Schönert[m], H. Simgen[i], M. Skorokhvatov[g], O. Smirnov[b], A. Sotnikov[b], S. Sukhotin[g], Y. Suvorov[s,g], R. Tartaglia[e], R.B. Vogelaar[o], M. Wojcik[d], M. Wurm[t], O. Zaimidoroga[b], S. Zavatarelli[c], G. Zuzel[d]

[a] APC, Univ. Paris Diderot, CNRS/IN2P3, CEA/Irfu, Obs. de Paris Sorbonne Paris Cité, France
[b] Joint Institute for Nuclear Research, Dubna 141980, Russia
[c] Dipartimento di Fisica, Università e INFN, Genova 16146, Italy
[d] M. Smoluchowski Institute of Physics, Jagellonian University, Krakow, 30059, Poland
[e] INFN Laboratori Nazionali del Gran Sasso, Assergi 67010, Italy
[f] Kiev Institute for Nuclear Research, Kiev 06380, Ukraine
[g] NRC Kurchatov Institute, Moscow 123182, Russia
[h] Dipartimento di Fisica, Università degli Studi e INFN, Milano 20133, Italy
[i] Max-Plank-Institut für Kernphysik, Heidelberg 69029, Germany
[j] Dipartimento di Chimica, Università e INFN, Perugia 06123, Italy
[k] Physics Department, Princeton University, Princeton, NJ 08544, USA
[l] St. Petersburg Nuclear Physics Institute, Gatchina 188350, Russia
[m] Physik Department, Technische Universität München, Garching 85747, Germany
[n] Physics Department, University of Massachusetts, Amherst MA 01003, USA
[o] Physics Department, Virginia Polytechnic Institue and State University, Blacksburg, VA 24061, USA
[p] Lomonosov Moscow State University, Institute of Nuclear Physics, Moscow 119234, Russia
[q] Institut für Experimentalphysik, Universität Hamburg, Germany
[r] Department of Physics, University of Houston, Houston, TX 77204, USA
[s] Physics ans Astronomy Department, University of California Los Angeles (UCLA), Los Angeles, CA 90095, USA
[t] Eberhard Karls Universität Tübingen, Physikalisches Institut, auf der Morgenstelle 14, 72076 Tbingen, Germany

The main results of the solar Phase-I of the Borexino experiment are summarized and two recent results are presented: the evidence of the annual modulation of the interaction rate of ^{7}Be solar neutrinos and the recent data about the detection of geo-neutrinos.

XV Workshop on Neutrino Telescopes,
11-15 March 2013
Venice, Italy

*Speaker.

PoS(Neutel 2013)008

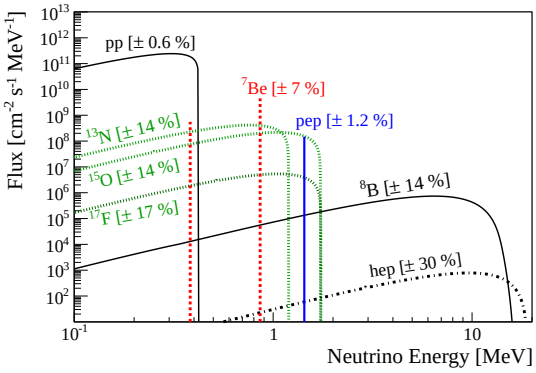

Figure 1: Energy spectrum of solar neutrinos from [1] (High Metallicity model). The numbers is parenthesis represent the theoretical uncertainties.

Solar ν	GS98 Flux High metallicity [cm^{-2}s^{-1}]	AGSS09 Flux Low metallicity [cm^{-2}s^{-1}]	e^- recoil end point [MeV]	GS98 rate [cpd/100 t]	AGSS09 rate [cpd/100 t]
pp	5.98 (1±0.006)	6.03 (1±0.006)	0.26	132.9 ± 1.9	133.2 ± 1.9
^{7}Be	5.00 (1± 0.07)	4.56 (1± 0.07)	0.66	48.5 ± 3.7	44.0 ± 3.2
pep	1.44 (1± 0.012)	1.47 (1± 0.012)	1.22	2.75 ± 0.05	2.81 ± 0.05
^{13}N	2.96 (1± 0.14)	2.17 (1± 0.14)	1.19		
^{15}O	2.23 (1± 0.15)	1.56 (1± 0.15)	1.73		
^{17}F	5.52 (1± 0.17)	3.40 (1± 0.16)	1.74		
CNO	5.24 (1± 0.21)	3.76 (1± 0.21)	1.74	5.26 ± 0.52	3.78 ± 0.39
^{8}B	5.58 (1± 0.14)	4.59 (1± 0.14)	17.72	0.44 ± 0.06	0.36 ± 0.05

Table 1: The solar neutrino flux, the expected neutrino interaction rate in Borexino and the end point of the electron energy recoil. We report the fluxes of neutrinos calculated with the high–metallicity standard solar model (GS98) [1] and the ones obtained with the low–metallicity model (AGSS09) [2]. The fluxes are given in units of 10^{10}(pp), 10^{9}(^{7}Be), 10^{8} (pep, 13^{N}, ^{15}O) and 10^{6} (^{8}B, ^{17}F). The CNO flux is the sum of the ^{13}N, ^{15}O and ^{17}F fluxes. The rate calculations are based on the MSW–LMA oscillation parameters from [8].

1. Introduction

The main goal of the Borexino detector is the measurement of the spectrum and flux of low energy solar neutrinos. After several years since the beginning of their detection, solar neutrinos are still a source of important information in astrophysics and in neutrino physics. The standard solar model predicts the spectrum of solar neutrinos as it is shown in fig. 1 but the value of the flux of the various components is still a subject of scientific debate in the astrophysics community. The so called High Metallicity [1] and Low Metallicity [2] models predict different fluxes, in particular for the neutrinos of the subdominant CNO cycle. The precise measurement of the neutrinos fluxes, in particular of the CNO, can help to discriminate between these models. Table 1 summarizes the predictions of the two models and the expected interaction rates of the neutrinos in Borexino.

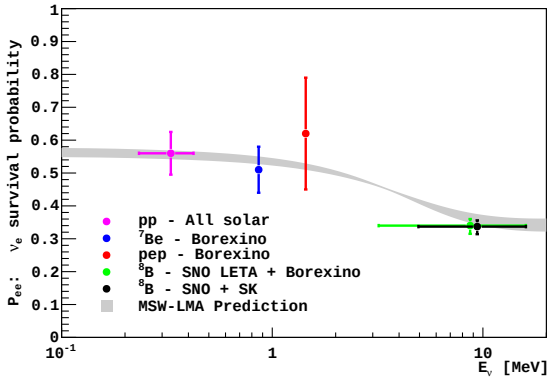

Figure 2: Electron neutrino survival probability as a function of energy in the LMA-MSW scenario.

Solar neutrinos offer also a way to deeply probe the models about neutrino oscillation and eventually to single out or to constrain hypothesis about not standard neutrino interactions [10]. The Sun produces electron neutrinos but they reach the Earth as a mixture of all flavours. Matter oscillations in the Sun play a key role (MSW effect) in the oscillation process. The resulting electron neutrino survival probability P_{ee}, according to the LMA-MSW solution of the oscillation scenario, is shown in figure 2 together with the results of the solar neutrinos measurements. Non standard interactions significantly modify the shape of this curve. The precise measurement of all the solar neutrinos fluxes is a powerful tool to confirm or not the prediction of the LMA-MSW scenario.

Borexino is collecting data since May 2007 in the Laboratory Nazionali del G. Sasso (Italy). The principle of the detector design is very simple: it basically consists of a of $\sim$278 ton of organic liquid scintillator contained within a sphere of 4.25 m diameter, viewed by 2200 photomultipliers and shielded against the external radioactivity. Details of the detector are described in [14]. What makes this instrument extremely powerful for performing solar neutrino spectroscopy below 2 MeV, are the unprecedented low levels of background that have been achieved after several years of research and efforts. Neutrinos interact through elastic scattering with electrons in the liquid scintillator target. There is no particular signature that allows to distinguish between neutrino induced events and background due to the radioactive decay of isotopes contaminating the scintillator and the surrounding materials. The expected solar neutrino event rate of few tens or few events per day in 100 tons sets the requirements about the needed radiopurity. The true signal is extracted from the background mainly fitting the energy spectrum of the detected events and then the possibility to identify and measure the signal from the solar neutrinos relies on achieving very low background rates.

Before performing the fit procedure there are a few powerful handles allowing to discriminate the signal from the background. One of this is the fast time response of the scintillator that allows to reconstruct the position of the events and thus to define a wall less fiducial volume where the background events are sufficiently suppressed. We have defined different fiducial volumes depending on the particular signal that we wanted to extract as it results in table 2. A second important

Analysis	R_{max} [m]	z_{min} [m]	z_{max} [m]	Volume [m^3]	Mass [ton]	N_{e^-} $\times 10^{31}$
^{7}Be	3.021	−1.67	1.67	86.01	75.47	2.835
pep–CNO	2.8	−1.8	2.2	81.26	71.30	2.679
^{7}Be day–night asymmetry	3.3	-3.3	3.3	151.01	132.50	4.978
^{7}Be annual modulation (mean)				161.64	141.83	5.329

Table 2: Definition of the fiducial volumes used in the different solar neutrino studies.

handle is the pulse shape discrimination due to the different time response of the scintillator to the energy deposit of different type of particles. This feature allows to suppress events due to α decay and also to discriminate between energy deposit due to electrons (or gamma) and positrons. We call solar Phase-I the period from May 2007 to May 2010 during which we first detected and then precisely measured the flux of the ^{7}Be solar neutrinos, ruled out any significant day- night asymmetry of their interaction rate, made the first direct observation of the pep neutrinos, and set the tightest upper limit on the flux of CNO neutrinos. These results are summarized in section 2.

During this period we also set limits about rare processes [11] and we detected geo neutrinos [12]. During Phase-I we have identified the main sources of background due to the residual radioactive contamination of the scintillator; we have calibrated the detector inserting radioactive sources in the active volume [13] and we have established the analysis procedures. All these aspects are widely discussed in [15]. A recent result obtained with the data of the Phase-I (also reported in [15]) is the evidence of the annual modulation of the interaction rate of the ^{7}Be solar neutrinos due to the yearly variation of the distance between the Earth and the Sun. This modulation confirms the solar origin of the signal. Section 3 is devoted to recall the main features of this analysis.

After May 2010 we began a series of procedures to purify the scintillator aiming to further reduce the background with the goal of increasing the sensitivity of the solar neutrino detection. We call solar Phase-II the data taking period after the end of this purification campaign. The period during the purification still consists of data usable for several measurements: in particular for the search of geo-neutrinos. Recent results about this subject, now published in [23], will be reviewed in section 4.

2. Summary of main results obtained during the solar Phase-I

The energy spectrum of the events passing a series a cuts aiming to eliminate muons and muons daughters, noise events and time correlated decays is shown in figure 3. This is one example of spectrum used to measure with 5% accuracy the interaction rate of ^{7}Be neutrinos. The figure shows the fit with solar neutrinos and the relevant background. The first measurement of the ^{7}Be interaction rate was published by Borexino after only few months of data taking [3] and an update was reported in [4]. The accuracy of those measurements was significantly improved in 2011 [5] using the results of the calibration campaign, a better understanding of the detector response, and increased statistics. The Phase-I data set has been used. It corresponds to 740.7 live days after cuts and to 153.6 ton $\times$ yr fiducial exposure. The resulting interaction rate is ($R^{^7Be}$ = 46.0 $\pm$ 1.5

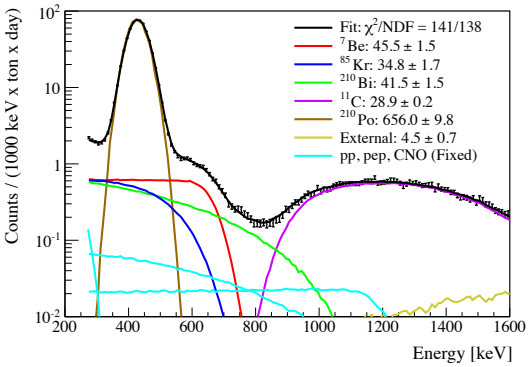

Figure 3: Example of fit of the energy spectrum obtained using the Monte Carlo method without α – β statistical subtraction. The values of the fitted parameters are [cpd / 100 t)].

(stat) $^{+1.5}_{-1.6}$ (syst)) counts/(day 100 tons) corresponding to a ν_e equivalent ^{7}Be solar neutrino flux of $(3.10 \pm 0.15) \times 10^{9}$ cm^{-2} s^{-1}. The measurement has been achieved cross checking the results obtained with two analysis procedures: one of them models the energy response of the detector through analytical functions while the second one is based on ab initio Montecarlo simulation of the scintillation process, light propagation and collection. Both methods are calibrated using the data obtained with the radioactive sources. The same sources allowed also to establish the precision of the position reconstruction algorithm.

The pulse shape discrimination feature of the scintillator has been used to perform a statistical subtraction of the events due to the α decay of the ^{210}Po: these events are clearly visible in fig.3. The results obatined with and without statistical subtraction are consistent.

We have searched [6] for a possible asymmetry between the day and night ^{7}Be solar neutrino interaction rate. This asymmetry is expected in particular regions of the oscillation parameters or it could be a signal for non standard neutrino interaction. The day–night asymmetry A_{dn} of the ^{7}Be count rate is defined as:

$$A_{dn} = 2\,\frac{R_N - R_D}{R_N + R_D} \tag{2.1}$$

where R_N and R_D are the night and day ^{7}Be–neutrino count rates.

With the data collected in the same period used to measure the ^{7}Be neutrino interaction rate we have found a result well consistent with absence of asymmetry A_{dn}=-0.001$\pm$0.012(stat)$\pm$0.007(sys) [6]. The obtained A_{dn} value excludes the non standard scenario described in [7].

A remarkable consequence of this result emerges when a global analysis of the all the neutrino data is performed. We have shown that the regions of the oscillation parameters $\Delta m^2_{1,2}$ and $\tan^2\theta_{1,2}$ determined by the Borexino data combined with that of the others solar neutrino experiments single out the LMA region even without including in the global analysis the results of the KamLAND experiment about reactor antineutrinos. The LMA solution is thus obtained without assuming the validity of CPT symmetry.

The detection of pep and CNO neutrinos is more challenging than the ^{7}Be one, as their expected interaction rates are $\sim$10 times lower. The pep neutrino interaction rate and the limits of the CNO neutrino rate have been determined [9] by extending the fitting procedure used to evaluate

the ^{7}Be interaction rate: we have used a multivariate approach in which the energy spectra were simultaneously fit together with the distribution of a proper pulse shape parameter and with the radial distribution of events. We expect a spatial not uniform distribution for events due to external background. The dominant background in the 1–2 MeV energy range, the cosmogenic, β^+-emitter ^{11}C is reduced through 1) correlation with the parent muon and 2) pulse shape discrimination.
The cosmogenic production of ^{11}C is associated with neutrons production. Up to 95% of the ^{11}C background can be reduced by performing space and time vetoes after coincidences between ^{11}C, the cosmogenic neutrons and the parent muon (Three-Fold Coincidence, TFC), relying on the reconstructed position of the neutron-capture γ-ray and the track of the muon [16]. The rejection criteria were chosen to obtain the optimal compromise between ^{11}C rejection and preservation of fiducial exposure, resulting in a ^{11}C rate of 9±1% of the original, with a 51.5% loss in the fiducial exposure. The resulting spectrum corresponds to a fiducial exposure of 20409 ton·day, consisting of data collected between Jan 13th, 2008 and May 9th, 2010.

After the TFC suppression, residual ^{11}C is still a significant background in the energy region of interest. We took advantage of the observed pulse-shape differences between e^- and e^+ in organic liquid scintillators [20] to discriminate between 11C β^+ decays and e^- induced scintillations. The delayed scintillation observed for ^{11}C is mostly attributed to the formation of ortho-positronium in a fraction of the decays, whose lifetime is comparable (∼ns) to the decay time of the fastest component in organic liquid scintillators. An optimized pulse shape parameter able to discriminate between e^+ and e^- has been built using a boosted-decision-tree algorithm trained with TFC-selected 11C events (e^+) and events selected by the fast ^{214}Bi-^{214}Po decay coincidence (e^-). The result about the pep neutrinos interaction rate is 3.1±0.6(stat)±0.3(sys) counts/(day 100 tons) corresponding to a solar flux of $1.6 \pm 0.3\ 10^8\,\mathrm{cm}^{-2}\mathrm{s}^{-1}$. Due to the similarity between the electron-recoil spectrum from CNO neutrinos and the spectral shape of ^{210}Bi, whose rate is ∼10 times greater, we can only provide an upper limit on the CNO neutrino interaction rate. The 95% C.L. limit on the flux has been obtained from a likelihood ratio test, with the pep neutrino rate fixed to the Standard Solar Model prediction. The result is that the flux is <7.9 counts/(day 100t). The ratio between this result and the standard solar model prediction is <1.5.

3. Annual modulation of the ^{7}Be solar neutrinos interaction rate

Due to the slight eccentricity $\varepsilon = 0.01671$ of the Earth's orbit around the Sun the flux Φ_E of solar neutrinos reaching the Earth is time dependent:

$$\Phi_E(t) = \frac{R_{Sun}}{4\pi r^2(t)} \simeq \frac{R_{Sun}}{4\pi r_0^2}\left(1 + 2\varepsilon cos\left(\frac{2\pi t}{T}\right)\right) \tag{3.1}$$

where R_{Sun} is the neutrino production rate at the Sun, T is one year, $r(t)$ is the time dependent Earth to Sun distance and r_0 is its mean value. The peak–to–peak amplitude of the modulation is $\simeq 7\%$. The detection of this annual modulation provides a strong confirmation of the solar origin of the signal.

The spectral fit analysis used to measure the interaction rate of the ^{7}Be neutrinos is not optimal to disclose the modulation. With only three-years of data, there is not sufficient statistics for independent spectral fit in sub periods of the live time giving results with a statistical error small

enough to identify the annual modulation. For this reason we have implemented three alternative analysis approaches, optimized for their sensitivity to the modulation. In all of them, the starting point is the definition of a set of time bins t_k and of the corresponding normalized event rate $R(t_k)$, obtained by selecting all events falling within a given energy window and by applying a proper time normalization. In the first approach (fit of the rate versus time) we fitted $R(t_k)$ as a function of time searching for the sinusoidal signal of Eq. 3.1.

The second approach consists of using the Lomb Scargle method [17], [18] to extract the periodical signal from $R(t_k)$. The Lomb Scargle method is an extension of the Fast Fourier Transform, well suited in our conditions since it allows to account for data sample not evenly distributed in time (there are in fact time gaps in the Borexino data taking) and it determines the statistical significance of the identified periodicities.

The third method is the Empirical Mode Decomposition (EMD) [19]. Details about all the methods are in [15]: the results obtained with the 3 procedures are consistent and in agreement with the expectation.

The two main challenges of this analysis were enlarging the fiducial volume as much as possible to increase the statistical significance of the modulated data and studying the time stability of the background. The major concern is related to the observed time variations of the ^{210}Bi rate. At the start of data taking, following the initial filling of the detector, the ^{210}Bi rate was measured as (10 ± 6) counts/(day 100 tons). However, over time, the ^{210}Bi contamination has been steadily increasing and at the start of May 2010 the rate was $\simeq$75 counts/(day 100 tons). The reason for this increase is currently not fully understood but it seems correlated with operations performed on the detector.

The simplest analysis is the fit of the rate versus time. The data selected in the 145 tons FV are grouped in bins in 60-days long and fitted with

$$R(t) = R_0 + R_{\mathrm{Bi}} e^{\Lambda_{\mathrm{Bi}} t} + \bar{R}\left[1 + 2\varepsilon \cos\left(\frac{2\pi t}{T} - \phi\right)\right] \tag{3.2}$$

R_0 is the background rate not depending on time, the exponential term describes the time variation of the ^{210}Bi rate and $\bar{R}$ is the neutrino interaction rate. The amplitude of the modulation and the average neutrino rates returned by the fit are in agreement to within 2σ with the expected ones. The period and the phase are close to the theoretical values of 1 year ± 0.07 and 0 days ± 14 respectively.

To perform the analysis with the Lomb Scargle method we used data grouped into 10-day bins. Before performing the frequency analysis we had to implement a correction to the data which consists in subtracting from them the exponential trend obtained studying the ^{210}Bi rate. This trend causes the Lomb-Scargle algorithm to misidentify the annual peak.

The significance of the Lomb-Scargle analysis is studied with a Monte Carlo simulation and is shown in the right plot of Fig. 4. The red distribution corresponds to the null hypothesis (absence of modulation) and the blue one corresponds to 10^4 simulations of the annual modulation signal plus expected backgrounds in the considered volume. The Spectral Power Density obtained with our data in the 145 t FV is 7.961 at 1 year (see the left plot of Fig. 4). As the figure shows, this value represents an evidence of the annual modulation signal with a significance higher than 3 sigma. The comparison with the expected distribution in presence of signal shows a consistency of 11.69 %.

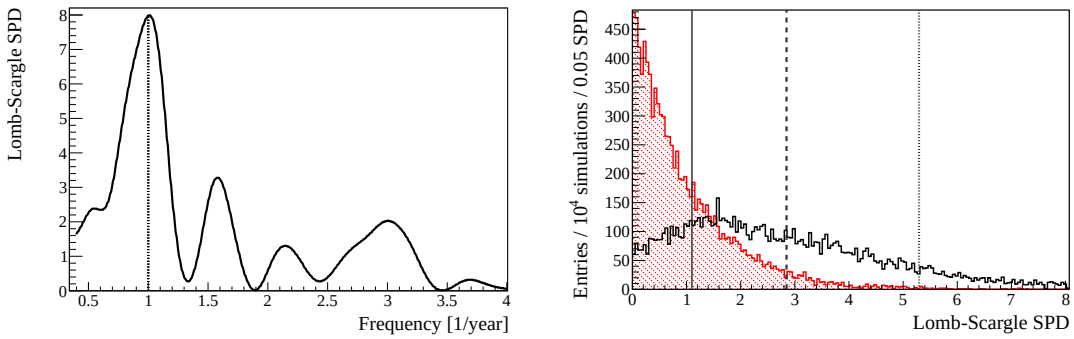

Figure 4: Left: Lomb-Scargle periodogram for ν data. The Spectral Power Density at 1-year is identified to be 7.961, as indicated by the vertical line. Right: distributions of the Lomb-Scargle Spectral Power Density at the frequency corresponding to 1 year for 10^4 simulations of a 7% solar neutrino annual flux modulation with realistic background (black line) and the same number of white-noise simulations (background without any signal) (red area). Indicated with vertical lines are the sensitivity thresholds of 1σ (solid), 2σ (dashed), and 3σ (dotted) C.L. with corresponding detection probabilities of 81.62, 43.54, and 11.68%, respectively.

4. Geo-neutrinos

Geo–neutrinos are electron anti–neutrinos produced mainly in β decays of ^{40}K and of several nuclides in the chains of long–lived radioactive isotopes ^{238}U and ^{232}Th, which are naturally present in the Earth. By measuring the geo–neutrino flux from all these elements, it is in principle possible to deduce the amount of the radiogenic heat produced within the Earth, an information facing large uncertainty and being of crucial importance for geophysical and geochemical models. The first experimental investigation of geo–neutrinos from ^{238}U and ^{232}Th was performed by the KamLAND collaboration [21, 22], followed by their observation with a high statistical significance of 99.997% C.L. by Borexino [12]. Here we summarizes the updates results of Borexino [23]. Additional results from Kamland are in [24]. In liquid scintillator detectors, $\bar{\nu}_e$ are detected via the inverse neutron β decay,

$$\bar{\nu}_e + p \rightarrow e^+ + n, \tag{4.1}$$

with a threshold of 1.806 MeV, above which lies only a small fraction of $\bar{\nu}_e$ from the ^{238}U (6.3%) and ^{232}Th (3.8%) series. Geo–neutrinos emitted in ^{40}K decay cannot be detected by this technique. The positron created in this reaction promptly comes to rest and annihilates producing a prompt signal with a visible energy of $E_{\rm prompt} = E_{\bar{\nu}_e} - 0.784\,$MeV. The emitted free neutron is typically captured on protons, resulting in the emission of a 2.22 MeV de–excitation γ ray, providing a delayed coincidence event. The mean neutron capture time in Borexino was measured with an AmBe neutron source to be $\tau = (254.5 \pm 1.8)\,\mu$s. The characteristic time and spatial coincidence of prompt and delayed events offers a clean signature of $\bar{\nu}_e$ detection, further suppressing possible background sources. The updated Borexino result has been obtained with the data collected between December 2007 and August 2012, corresponding to 1352.60 days of live time. The fiducial exposure after all cuts is (613 ± 26) ton $\times$ year or $(3.69 \pm 0.16) \times 10^{31}$ proton $\times$ year. Details of the event selection procedure are described in [23]. The only relevant background is due to reactor antineutrinos. Since there are no nuclear plants in Italy, the LNGS site is well suited for

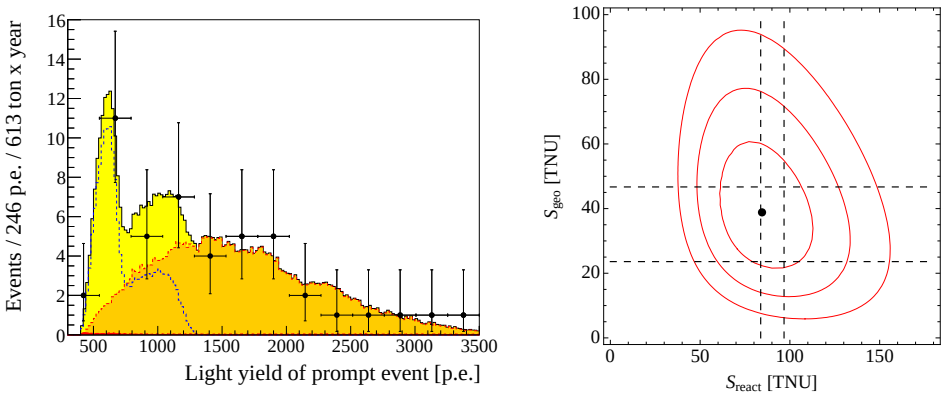

Figure 5: Left: light yield spectrum of the 46 prompt golden anti–neutrino candidates and the best fit. The yellow area isolates the contribution of the geo–$\bar{\nu}_e$ in the total signal. Dashed red line/orange area: reactor–$\bar{\nu}_e$ signal from the fit. Dashed blue line: geo–$\bar{\nu}_e$ signal resulting from the fit. The contribution of background others than that of the reactors is almost negligible and is shown by the small red filled area in the lower left part. The conversion from p.e. to energy is approximately 500 p.e./MeV. Right: 68.27, 95.45, and 99.73% C.L. contours for the geo–neutrino and the reactor anti–neutrino signals and comparison to expectations.

geo neutrinos detection. We have estimated the background due to 446 nuclear reactors situated in various sites in the world after collecting from the International Atomic Energy Agency (IAEA) the data about their power and monthly load factor. The number of expected reactor $\bar{\nu}_e$ candidates is N_{react} = (33.3 ± 2.4) events for the exposure of (613 ± 26) ton × yr after cuts including neutrino oscillations.

We have identified 46 golden anti–neutrino candidates passing all the selection criteria having uniform spatial and time distributions. The expected number of background events due to sources different from the reactor is only (0.70 ± 0.18). We have performed an unbinned maximal likelihood fit of the light yield spectrum of our prompt candidates. The weights of the geo–neutrino (Th/U mass ratio fixed to the the chondritic value of 3.9 and the reactor anti–neutrino spectral components were left as free fit parameters.

Our best fit values are $N_{\rm geo}$ = (14.3 ± 4.4) events and $N_{\rm react} = 31.2^{+7.0}_{-6.1}$ events, corresponding to signals $S_{\rm geo}$ = (38.8 ± 12.0) TNU[1] and $S_{\rm react} = 84.5^{+19.3}_{-16.9}$ TNU. The measured geo–neutrino signal corresponds to overall $\bar{\nu}_e$ fluxes from U and Th decay chains of ϕ(U) = (2.4 ± 0.7) × 10^6 cm^{-2} s^{-1} and ϕ(Th) = (2.0 ± 0.6) × 10^6 cm^{-2} s^{-1}. From the ln$\mathscr{L}$ profile, the null geo–neutrino measurement has a probability of 6 × 10^{-6}. The data and the best fit are shown in the left plot of Fig. 5 while the right plot shows the 68.27, 95.45, and 99.73% C.L. contours for the geo–neutrino and the reactor anti–neutrino signals in comparison to expectations. The signal from the reactors is in full agreement with the expectations of (33.3 ± 2.4) events in the presence of neutrino oscillations. The statistical uncertainty about the geo neutrinos data still does not allow to clearly single out specific models about the interior of the Earth. However their detection is a great success of the low background experiments and the interest in this field is growing over the years.

[1] 1 TNU = 1 Terrestrial Neutrino Unit = 1 event / year / 10^{32} protons

5. Conclusions and perspectives

The purification campaign of the scintillator has given very encouraging results: the count rate due to ^{85}Kr is now consistent with zero while the contribution of ^{210}Bi has decreased from the initial value of 70 cpd/100 t to about 20 cpd/100 t. The limit about the concentration of ^{238}U and ^{232}Th in the scintillator measured counting time correlated events in the decay chains and assuming saecular equilibrium are 9.7 10^{-19} g/g and 2.9 10^{-18} g/g both at 95 % C.L. There is a room for new exciting results about solar neutrinos detection in the next future.

References

[1] A.M. Serenelli, W.C. Haxton, and C. Peña-Garay, Astrophys. J. **743** (2011) 24

[2] M. Asplund et al., Astrophys. J. Lett. **705** (2009) L123

[3] C. Arpesella. et al. (Borexino Collaboration), Phys. Lett. B **658** (2008) 101.

[4] C. Arpesella et al. (Borexino Collaboration), Phys. Rev. Lett. **101** (2008) 091302

[5] G. Bellini et al. (Borexino Collaboration), Phys. Rev. Lett. **107** (2011) 141302

[6] G. Bellini et al. (Borexino Collaboration), Phys. Lett. B **707** (2012) 22.

[7] P. C. de Holanda, JCAP 0907, 024 (2009)

[8] K. Nakamura et al. (Particle Data Group), The Review of Particle Physics, J. Phys. G. **37** (2010) 075021

[9] G. Bellini et al. (Borexino Collaboration), Phys. Rev. Lett. **108** (2012) 051302

[10] A. Friedland et al., Phys. Lett. B **594** (2004) 347; S. Davidson et al., J. High Energy Phys. 03 (2003) 011; P. C. de Holanda and A.Yu. Smirnov, Phys. Rev. D **69** (2004) 113002; A. Palazzo and J.W.F. Valle, Phys. Rev. D **80** (2009) 091301

[11] G. Bellini et al. (Borexino Collaboration) Phys. Rev. D **85** (2012) 092003; G. Bellini et al. (Borexino Collaboration) Phys. Rev. C **81** (2010) 034317

[12] G. Bellini et al. (Borexino Collaboration), Phys. Lett. B 687 (2010)

[13] H. Back et al. (Borexino Collaboration), JINST 7 10 (2012) P10018

[14] G. Alimonti et al. (Borexino Collaboration), Nucl. Instrum. Methods Phys. Res. A **600** (2009) 568

[15] G. Bellini et al., (Borexino Collaboration) arXiv:1308.0443 (2013) (submitted to Phys. Rev. D)

[16] .G. Bellini et al. (Borexino Collaboration), JINST **6** (2011) P05005

[17] N. R. Lomb, Astrophysics and Space Science **39** (1976) 447

[18] J. D. Scargle, Astrophys. J. **263** (1982) 835

[19] N.E. Huang et al., Proc. R. Soc. Lond. A **454** (1998) 903

[20] D. Franco, G. Consolati and D.Trezzi, Phys. Rev. C **83** (2011) 015504

[21] T. Araki et al. (KamLAND Collaboration), Nature 436 (2005) 499.

[22] S. Abe et al. (KamLAND Collaboration), Phys. Rev. Lett. 100 (2008) 221803

[23] G. Bellini et al. (Borexino Collaboration), Phys. Lett. B 722 4-5 (2013) 295

[24] A. Gando et al., Phys. Rev. D 88 033001 (2013)